

Influence of the slag/pool interface on the solidification in an Electro-slag remelting process

Abdellah Kharicha^{1,a}, Wolfgang Schützenhöfer², Andreas Ludwig³ and Gerhard Reiter²

¹ Christian Doppler Laboratory for Multiphase Modeling of Metallurgical Processes, University of Leoben, A-8700 Franz-Josef Str. 18, Leoben, Austria

² Böhler Edelstahl GmbH & Co KG, Kapfenberg, Austria

³ University of Leoben, Leoben, AUSTRIA

^aabdellah.kharicha@notes.unileoben.ac.at

Keywords: ESR, remelting, slag, simulation, solidification, VOF, magnetohydrodynamic, electric current, flow, CFD, Joule heating, interface tracking, porosity, enthalpy.

Abstract. The Electro-Slag-Remelting (ESR) is an advanced technology for the production of components of e.g. high quality steels. In the present study a comprehensive computational model using the VOF technique for the prediction of the slag/pool interface is presented for axisymmetric and steady state conditions. In this model the distribution of the electric current is not constant in time, but is dynamically computed according to the evolution of the slag and steel phase distribution. The turbulent flow, created by the Lorentz and buoyancy forces, is computed by solving the time-averaged mass and momentum conservation equations. The turbulence effect is modelled by using a $k-\epsilon$ model. Two numerical simulations were performed, one assuming a flat interface, and a second leaving the interface free to find an equilibrium shape. The results are then analysed and compared for both cases.

Introduction

The Electro-Slag-Remelting (ESR) is an advanced technology for the production of components of e.g. high quality steels. An alternating current (AC) is passed from a conventionally melted and cast solid electrode through a layer of molten slag to the baseplate (Figure 1). Because of the electrical resistivity of the slag, Joule heating is generated and the slag transfers this energy to both ingot and mould surfaces and to the melting electrode tip. The molten metal produced in the form of droplets or a continuous stream passes through the slag and feeds a liquid pool which then solidifies nearly directionally. The slag and the ingot are contained in a water cooled copper mould. As also the baseplate is water cooled, a heat flow regime is imposed that gives controlled solidification, and this results in an improved structure characteristic of ESR ingots. The present investigation aims to create a numerical model that can predict all these features with a minimum of assumptions. In terms of modelling, the ESR process is a multiphase magnetohydrodynamic (MHD) system with heat and mass transfer. Simulations [1-9] can be found in literature, but due to the complexity of the system and due to the computational restrictions, several assumptions and simplifications are necessary.

One of the assumptions consists in assuming a flat slag/liquid pool interface. A previous work [8] using a VOF model has shown that the interface between a layer of slag and steel layer in a cylindrical cavity is highly coupled with the distribution of the electric current. The results were produced only for a basic DC field and by considering only the Lorentz force. The temperature distribution was not calculated so that the influence of the buoyancy and the mushy zone on the momentum equations was not taken into account. Here the same VOF model has been further developed to calculate the temperature and the solidification fields resulting from the application of an AC current. The objective of the present work is not to predict the solidification front, but to illustrate the consequences of a curved the slag/steel pool interface, in particular on the Joule

heating distribution. For that it is necessary to know roughly the bottom limit of the fluid domain. Therefore we decided to use an enthalpy-porosity model to approximate the pool profile. Two calculations were performed, one assuming a flat slag/steel interface, and a second leaving the interface free to find an equilibrium shape.

The Numerical Model

The axisymmetric calculation domain is presented in figure. 1. An electrode is put in contact with a cylindrical container filled with a layer of liquid slag and a larger layer of liquid steel. The properties of both steel and slag as the density (ρ), dynamical viscosity (μ), and electrical conductivity (σ) are assumed to be temperature dependant. The magnetic permeability (μ_0) is the same everywhere and equal to the vacuum magnetic permeability. The electrode supplies a total 5Hz AC current of 5000 Amperes. Table 1 lists typical physical properties of the alloy, the slag, the geometry and the operating conditions used for the present simulations.

The VOF technique. The well known VOF method provides the possibility of tracking immiscible interfaces that are of interest for the present study. The VOF model is a surface-tracking technique applied to a fixed Eulerian mesh. It is designed for two or more immiscible fluids where the position of the interface between the fluids is of interest. A single set of momentum equations is shared by the fluids, and the volume fraction of each of the fluids in each computational cell is tracked throughout the domain.

In the VOF method the motion of the interface between immiscible liquids of different properties is governed by a phase indicator, the so-called volume fraction f , and an interface tracking method. The volume fraction f_k is equal to 0 outside of liquid k , and equal to 1 inside. According to the local value of f , appropriate properties and variables are assigned to each control volume within the domain. A standard advection equation governs the evolution of f_k for a given flow field \vec{u} :

$$\frac{Df}{Dt} = 0 \Rightarrow \frac{\partial f}{\partial t} + \nabla \cdot (\vec{u}f) = 0. \quad (1)$$

In a two phase system the properties appearing in the momentum equation are determined by the presence of the component phase in each control volume. The average values of density, viscosity and electric conductivity are interpolated by the following formulas

$$\rho = \rho_1 + f_2 (\rho_2 - \rho_1), \quad \mu = \mu_1 + f_2 (\mu_2 - \mu_1) \quad \text{and} \quad \sigma = \sigma_1 + f_2 (\sigma_2 - \sigma_1), \quad (2)$$

where the subscript 1 and 2 indicate the slag and steel phase, respectively. The same procedure is used for all other properties of the fluid, such as the heat capacity C_p , heat conductivity k and the thermal expansion coefficient β . The implicit version of the VOF technique was used for the present calculations. The surface tension is supposed to play a role on much smaller scales than the dimensions of the present geometry, so that it is neglected.

Electromagnetics. The imposed vertical current is distributed over the entire domain according to the distribution of the slag and steel phase. Whereas there exist a radial and an axial component for the electric current, there is only a tangential component for magnetic field. For sinusoidal AC field,

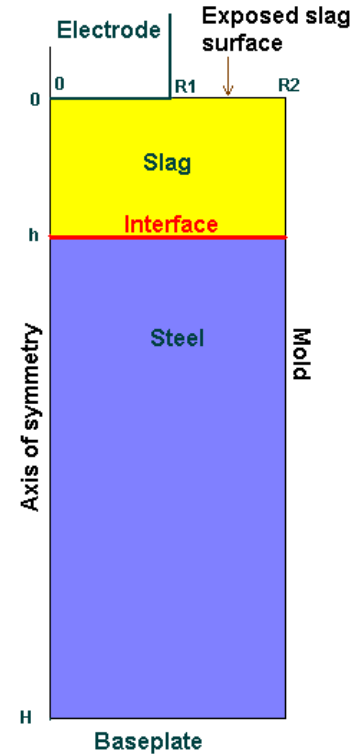


Figure 1. Calculation domain

we can express the magnetic field in complex notation: $H_\theta = \tilde{H}_\theta e^{i\omega t}$. The complex amplitude \tilde{H}_θ is a function of the position, and ω is the angular frequency. The equation to be solved can be expressed as:

$$\frac{\partial}{\partial r} \left(\frac{1}{\sigma \mu_0 \cdot r} \frac{\partial}{\partial r} (r \tilde{H}_\theta) \right) + \frac{\partial}{\partial z} \left(\frac{1}{\sigma \mu_0 \cdot r} \frac{\partial}{\partial z} (r \tilde{H}_\theta) \right) = i \omega \tilde{H}_\theta \quad (3)$$

The resolution is performed for both real and imaginary parts of this equation. Although the time is not present in Eq 3, the fact that σ can vary in time at one position (the slag/steel interface moves) makes \tilde{H}_θ also as a function of time.

Due to the very high difference between the electrical conductivity between the electrode and the slag, the radial current is assumed to be zero at the electrode. The same condition is used at the bottom baseplate: $\frac{\partial \tilde{H}_\theta}{\partial z} = 0$. From the Ampere's law, at the exposed slag surface and at the mould

the value of the magnetic flux is: $\tilde{H}_\theta(r) = \frac{I_0}{2\pi r}$, where I_0 denotes the amplitude of the total current, and r the radial distance to the rotating axis. Once the magnetic field is known, the electric current is obtained through: $\tilde{j} = \vec{\nabla} \times (\tilde{H}_\theta \vec{e}_\theta)$

Hydrodynamics. The two-phase buoyant fluid flow is modelled with the Navier-Stokes equation according to

$$\frac{D\rho}{Dt} \vec{u} = -\nabla p - \rho \vec{g} \beta (T - T_{Ref}) + \nabla \cdot ((\mu + \mu_T)(\nabla \vec{u} + \nabla \vec{u}^T)) + S + \mu_0 \text{Re} \left(\frac{1}{2} \tilde{j} \times \tilde{H}_{\theta \text{Conjugate}} \right). \quad (4)$$

Here p represents the pressure and g the gravitational acceleration. The effect of turbulent mixing is taken into account through the turbulent viscosity μ_T . For this a k- ϵ model is used. The Boussinesq approximation is used for determining the buoyancy force. S is the momentum sink at the mushy zone, see next section for more details. The last term on the right hand side of Eq.4 represents the Lorentz force. The no-slip boundary condition is imposed at all boundaries except at the exposed slag surface where a total slip condition is used.

The Energy equation. The temperature distribution is governed by the energy conservation equation:

$$\frac{D\rho}{Dt} C_p T = \nabla \cdot ((k + k_T)(\nabla T)) + \text{Re} \left(\frac{1}{2\sigma} \tilde{j} \times \tilde{j}_{\theta \text{Conjugate}} \right) - \rho \vec{u} L \vec{\nabla} \cdot \lambda \quad (5)$$

Where L is the latent heat, and k_T the turbulent thermal conductivity. The lever rule is used to define the liquid fraction $\lambda = (T - T_{Solidus}) / (T_{Liquidus} - T_{Solidus})$. Once the liquid fraction is determined, the momentum sink in (Eq. 4) is then calculated according to:

$$S = -A \frac{(1 - \lambda)^2}{\lambda^3} \vec{u} \quad (6)$$

Where A is the mushy zone constant, taken equal to 10^5 . Joule heating created by the current is taken into account only in the slag domain. Similarly the latent heat released appears as source term acting in the steel region only.

The present study performs analysis of the ESR process for very small melt rate of 1.9 kg/min. The

total heat lost at the electrode is set to $\dot{m} \left(L + \int_{ambient}^{Liquidus} C_p dT \right)$. At the exposed slag surface heat is lost

through radiation. The heat transported by the droplets to the liquid pool, is taking into account through a special heat source at the Slag/steel interface. The bottom surface is treated as an outflow boundary and conditions at this surface are calculated by extrapolation from within the domain. The most important boundary conditions on the energy transport are those at the mold. At a boundary node at the mould the boundary condition depends on whether the boundary cell is filled with slag or steel. As we do not model the solidified slag layer we can impose the slag liquidus temperature if the adjacent cell is filled with slag. At the height of the liquid pool there is a minimum in heat transfer from the ingot through the slag skin and mould to the cooling water. There a heat transfer coefficient of $\sim 1000 \text{ W/m}^2$ is used. The heat transfer coefficient across the ingot-mold shrinkage gap is much lower [7].

Results and Comments

Figures 2-4 represent the variations of the electromagnetic, hydrodynamic and thermal results in the r-z plane for the two cases considered. When the interface is imposed to be flat, the results agree with most of the previous simulations results found in the literature [1-7]:

1) The distribution of the electric current is mainly vertical, except at the extremity of the electrode and under the slag exposed surface (figure 2a.). This last zone corresponds also to the region where most of the Joule heating is released. Usually the ESR process uses 50 Hz AC currents, this induces a sensitive skin effect at the liquid steel region [6]. Here the use of a small AC frequency (5Hz) gives rise to a distribution closer to that of a DC current.

2) In figure 4 we can see that the flow is higher in the slag region compared to the liquid steel region [1-9]. Due to the high electric current density, the maximum velocity is located at the corner of the electrode. Nevertheless the flow in the steel pool is strong enough to generate a strong mixing at the origin of the quasi uniform temperature field in the liquid pool.

3) The slag is the hottest region (figure 3). The chosen heat boundary condition at the mold induces a parabolique pool profile. As usually found for small melting rate, the depth of the pool is of the same order than the slag depth [1-9].

In the case of a free interface, the main result is that at equilibrium the shape of the slag/melt interface is not flat but concave as found in [10]. The electric current distribution is highly modified compared to the case with a flat interface.

The curvature of the interface induces a strong horizontal component of the electric current (figure 2b). Nearly all the current coming from the electrode penetrates into the liquid steel at the top of the interface creating a new zone of high current density near the mold. This zone generates higher quantity of heat than the zone near the electrode, so that the total heat released through joule heating is much higher than that produced with a flat interface case.

Despite the high increase of the Joule heating, the temperature distribution is similar to that found for a flat interface. The maximum temperature is higher, i.e 1910 K for the flat interface and 2151 K

for the free interface. This result is due to the high mixing rate generated by the highly turbulent flow (high k_t).

The solidification of the steel started at the level of the interface, but become large only at a certain distance from the interface level (figure 4). The heat boundary conditions at the mold were not modified in order to see clearly the influence of the new Joule heating distribution. The iso-lines of temperature in the center are slightly shifted downward, making the pool deeper and a finer mushy zone.

The equilibrium of the forces is now totally different. An additional vertical Lorentz force is generated by the new horizontal component of the electric current. Nevertheless this flow conserves the same characteristics than in the imposed flat interface, except under the electrode where the velocity magnitude was found to be higher.

Conclusion

The present study describes a numerical model for the analysis of the magneto-hydrodynamics and heat transfer in the ESR process. The VOF model was used to track the interface. The aim of this work is to illustrate the consequences on the magneto-hydrodynamics and heat transfer if the slag/pool interface is left free to move. In the present configuration the interface was found to be concave. The Lorentz force and Joule heating distribution, and so the velocity and temperature field, are very different from the results found with a fixed flat interface. Keeping the same heat boundary conditions at the mold, the shape and the depth of the pool profile computed with the help of an enthalpy-porosity model was found to be different.

Several experiments using 5Hz AC field with different melt rate are planned. In the future, this model will be validated with measured temperatures in the mould and microstructural investigations of several ingots. Afterwards, this model will be applied with varying a large range of parameters, such as the diameter of the electrode and mold, the intensity and frequency of the imposed current, and the slag height

Acknowledgements

This project is funded by the “European Research Fund for Coal and Steel“ for which the authors kindly acknowledge.

References

- [1] M. Choudhary and J. Szekely. *Metall. Trans. B*, vol. 11B (1980), 439-453.
- [2] M. Choudhary and J. Szekely. *Ironmaking and Steelmaking* vol. 5 (1981) 225-232.
- [3] B. Hernandez-Morales and A. Mitchell. *Ironmaking and steelmaking*, 26 (6) (1999), p423-438
- [4] A. H. Dilawari and J. Szekely, *Metall. Trans. B*, (8B), (June 1997), 227-236.
- [5] G. Reiter, V. Maronnier, C. Sommitsch, M. Gäumann, W. Schützenhöfer, R. Schneider. *Proceeding in International Symposium on Liquid metal Processing and Casting, Nancy, (2003), 77-86.*
- [6] K. M. Kelkar, S. V. Patankar, A. Mitchel. *Proceedings of the 2005 International Symposium on Liquid Metal Processing and Casting, Santa Fe, New Mexicom USA, September 18-21 (2005), pages 137-144.*

- [7] L. Bertram, P. Schunk, S. Kempka, F. Spadafora and R. Minisandram, JOM (March 1998), 18-21.
- [8] K. Yu and Flanders. Proc. 1984 Vacuum Metallurgy Conference on Speciality Metals Melting and Processing. Pittsburgh, June 11 - 13th, (1984), 107-118
- [9] J. Szekely and A. Dilawari: Proc. 5th International Conference on Vacuum Metallurgy and Electroslag Remelting Processes, Munich, October 11th-15th, (1976), 157-160
- [10] A. Kharicha, A. Ludwig and M. Wu. *Materials Science & Engineering A* 413-414 (2005), 129-134.

Liquid Metal Steel W300	
Density	6800 kg/m ³
Viscosity	0.006 kg/m-s
Liquidus temperature	1752 K
Solidus temperature	1637 K
Latent heat of fusion	2.5*10 ⁵ J/kg
Specific heat, liquid	570 J/kgK
Thermal expan. coefficient	1.2 x 10 ⁻⁴ K ⁻¹
Thermal conductivity, liquid	35 W/mK
Thermal conductivity, solid	25 W/mK
Max. heat transfer coefficient	2500 W/m ² K
Electric conductivity, liquid	8.0x10 ⁵ (Ω-m) ⁻¹
Slag	
Density	2800 kg/m ³
Viscosity	2.5 x 10 ⁻³ kg/ms
Specific heat	1255 J/kg K
Thermal expan. coefficient	2.5x10 ⁻⁴ K ⁻¹
Thermal conductivity	6.0 W/mK
Thermal cond. slag skin	0.5 W/mK

Geometry	
Slag height (h)	125 mm
Electrode diameter (D1)	130 mm
Ingot Diameter (D2)	200 mm
Operating condition (experimental ESR)	
Electric current	5.0 Hz 5.0 kA
Melt rate	1.9 kg/min
Emissivity and temperature at the exposed slag surface	0.5 and 400.15 K
Cooling water temperature	300 K

Table 1: Physical properties and operating conditions used for the present study.

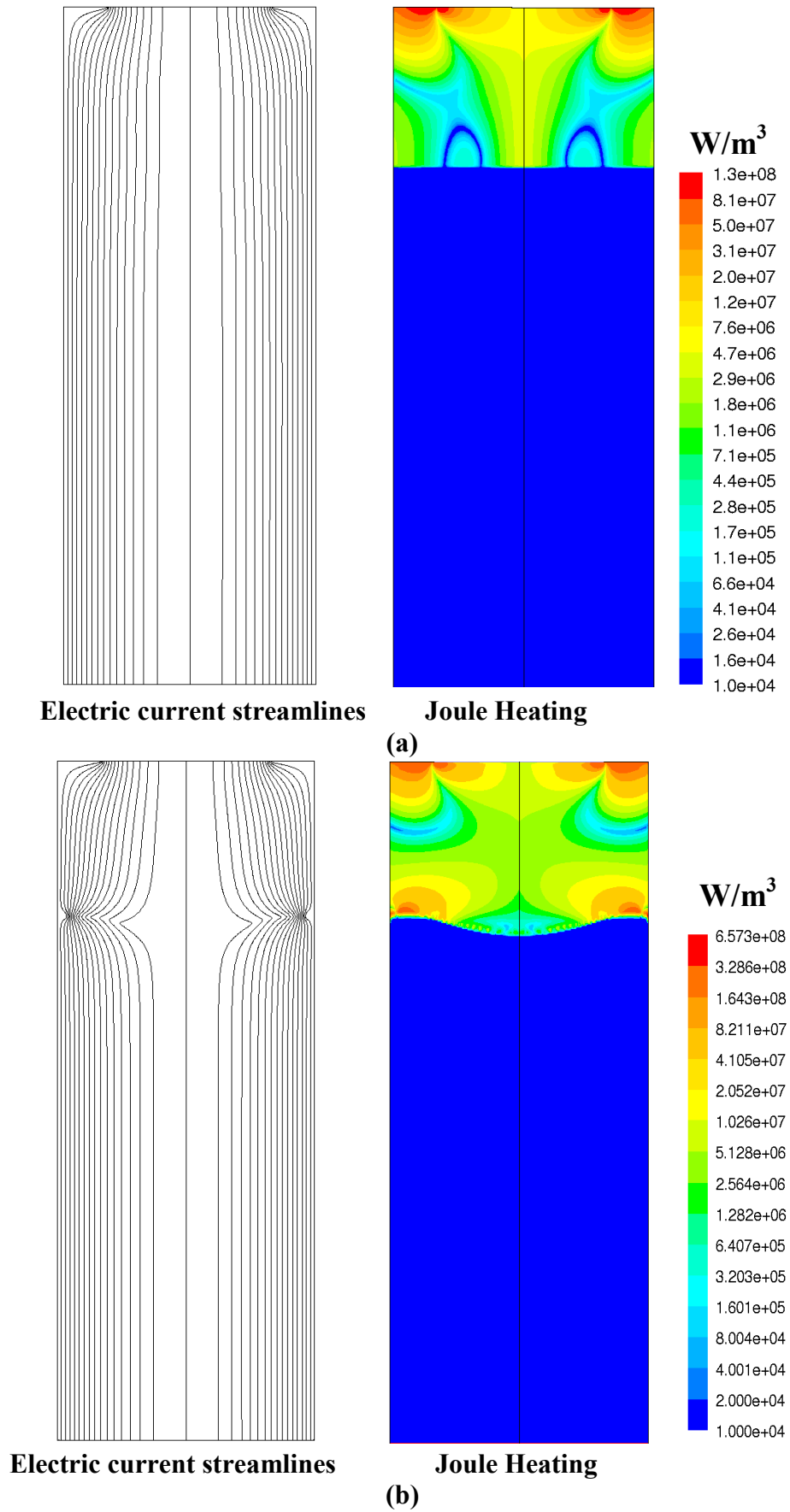


Figure 2. Field variations of electromagnetic quantities for the case of a imposed flat interface (a) and for the case of a free interface (b)

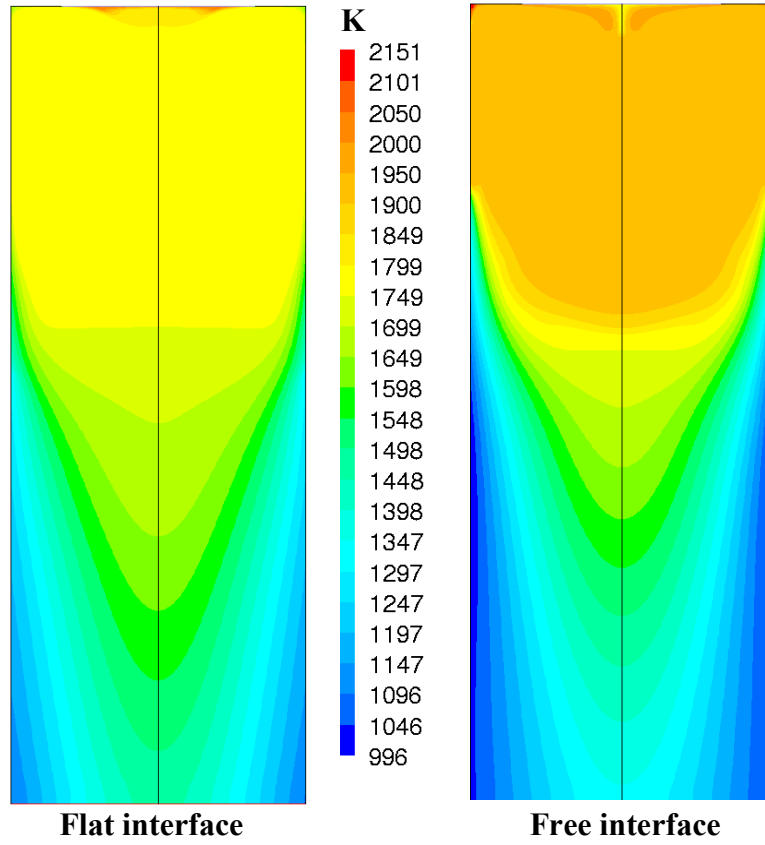


Figure 3. Field variations of temperature.

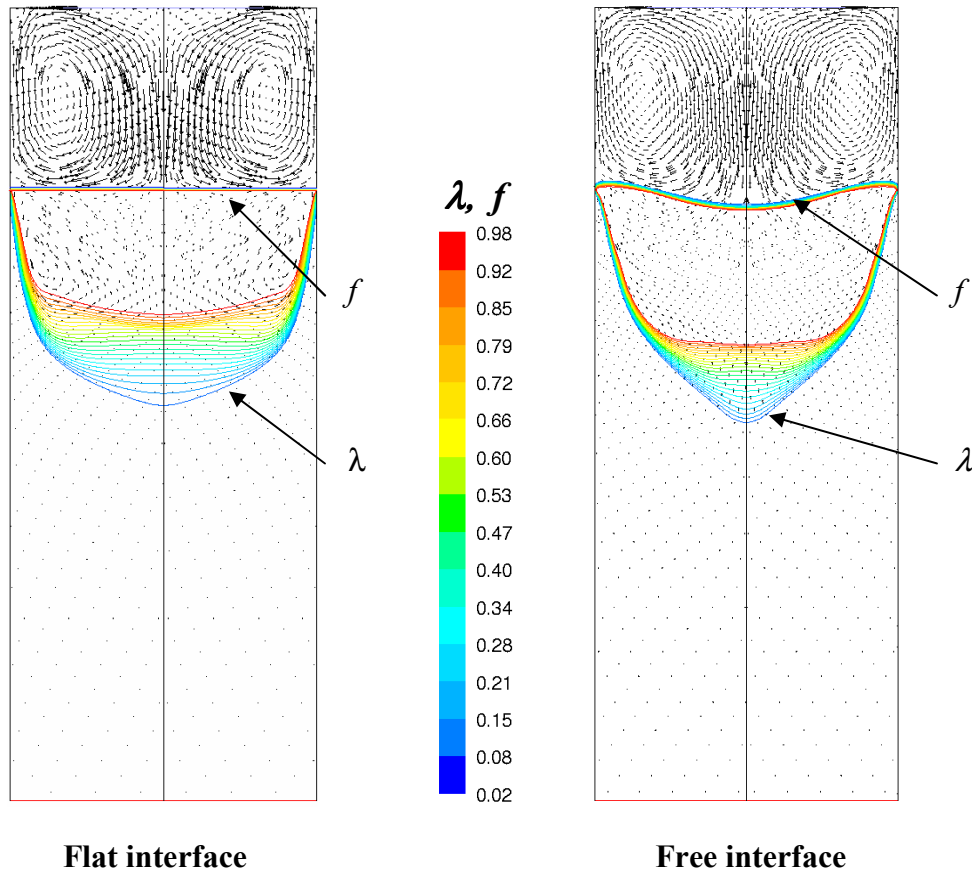


Figure 4. Field variations of velocity, liquid fraction λ and volume of steel fraction f .